

A multipolar approach to the interatomic covalent interaction energy

E. Francisco, D. Menéndez Crespo, A. Costales, A. Martín Pendás*

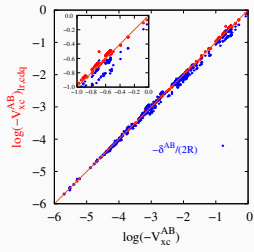
November 11, 2016

Abstract

Interatomic exchange-correlation energies correspond to the covalent energetic contributions to an interatomic interaction in real space theories of the chemical bond, but their widespread use is severely limited due to their computationally intensive character. In the same way as the multipolar (*mp*) expansion is customary used in biomolecular modelling to approximate the classical Coulomb interaction between two charge densities $\rho_A(\mathbf{r})$ and $\rho_B(\mathbf{r})$, we examine in this work the *mp* approach to approximate the interatomic exchange-correlation (*xc*) energies of the Interacting Quantum Atoms method. We show that the full *xc mp* series is quickly divergent for directly bonded atoms (1–2 pairs) albeit it works reasonably well most times for 1– n ($n > 2$) interactions. As with conventional perturbation theory, we show numerically that the *xc* series is asymptotically convergent and that, a truncated *xc mp* approximation retaining terms up to $l_1 + l_2 = 2$ usually gives relatively accurate results, sometimes even for directly bonded atoms. Our findings are supported by extensive numerical analyses on a variety of systems that range from several standard hydrogen bonded dimers to typically covalent or aromatic molecules. The exact algebraic relationship between the monopole-monopole *xc mp* term and the inter-atomic bond order, as measured by the delocalization index of the Quantum Theory of Atoms in Molecules, is also established.

Keywords: Chemical bonding, Atoms in Molecules, Covalent energy, Molecular energy partitioning, Electron delocalization ■

*Departamento de Química Física y Analítica. Facultad de Química. Universidad de Oviedo. 33006-Oviedo. Spain.



Interatomic or interfragment covalent energies in real space, as measured by the interacting quantum atoms (IQA) exchange-correlation energies (V_{xc}^{AB}) are shown to be well-approximated by a multipolar approximation if terms up to the charge-quadrupole interaction are retained (cdq). The cdq approximation improves considerably the performance of the zeroth-order approximation, in which V_{xc} is equal to the bond order (delocalization index, δ^{AB}) over the interatomic distance.

INTRODUCTION

The role of the quantum mechanical exchange-correlation (xc) energy as the basic glue binding together atoms and molecules has been clearly stressed in the past.¹ In the chemical literature, however, this insight is less well known. Although exchange-correlation functionals, for instance, are the essential ingredients in modern implementations of Density Functional Theory (DFT),² not much work has been devoted to examine the importance of the exchange-correlation energy itself in the theory of chemical bonding from the DFT viewpoint.³

Actually, almost all that is known about the chemical relevance of the xc energy has been derived in the last decade through the study of bonding in real or position space.^{4,5} With this term we gather together a number of techniques that are being actively explored⁶⁻⁸ which use orbital invariant reduced densities (or density matrices) to develop a new paradigm that may one day replace the standard molecular orbital approach.⁹ Usually, these techniques use a partition of real space into regions endowed with chemical meaning, be them atoms, bonds, cores, lone pairs, etc. In many cases, the space is divided using the topology induced by the gradient field of an orbital invariant scalar, like the electron density (which gives rise to the atomic partitioning of the quantum theory of atoms in molecules (QTAIM) developed by Bader and coworkers,¹⁰ or the electron localization function (that isolates core, bond and lone pair regions).^{11,12} When this topological tools are used we say that we are under the Quantum Chemical Topology umbrella.¹³

In the context of the QTAIM/QCT, we proposed a number of years ago an exact, general decomposition of the total molecular energy E into atomic and inter-atomic terms that we called the interacting quantum atoms (IQA) approach.^{4,5} All the expectation values of the standard Coulomb Hamiltonian that make up E are written in IQA as a sum of domain contributions, and E is obtained by adding atomic self-energies, which tend to the free atomic energies when the atoms that interact are sufficiently far apart, and pairwise additive interaction energies. The latter are composed of a classical term that depends only on classical electrostatic contributions, and an exchange-correlation energy, V_{xc} which accounts for all quantum mechanical effects. As we and others have shown over the years,^{14,15} the

classical part of the interaction measures its ionic component, while the V_{xc} energy is to be associated with its covalent counterpart.

In these years, the interatomic xc energy has become an important ingredient of any quantitative account of chemical bonding in position space.^{16,17} For instance, it has been shown to be intimately related to the appearance of the bond critical points of the QTAIM, leading to the concept of privileged exchange-correlation channels.¹⁸ It has also been used to reconstruct molecular graphs from purely energetic quantities,¹⁹ to shed light on new concepts like halogen bonding,^{20,21} to recover stereoelectronic effects,²² or to find new long-range electronic anomalies.²³

Interatomic V_{xc} energies are intimately linked to the delocalization or shared electron delocalization indices (DIs) used in the QTAIM, defined almost 40 years ago by Bader and Stephens.²⁴ These are obtained by directly integrating the xc density of very two different atomic domains and measure the number of shared pairs of electrons between them. They have been successfully used as real space generalization of the bond order concept, reducing to the Wiberg-Mayer^{25,26} bond orders if atomic domains are imagined to collapse onto their nuclei. In a sense, V_{xc} 's are the energetic counterparts of DIs, and both have been empirically found to correlate very well when a given couple of atoms is examined in different molecular environments.

The computational complexity of obtaining DIs is considerably smaller than that of calculating V_{xc} 's, since the former may be factorized into sums of products of atomic overlap matrices (3D numerical integrals), while the latter need, in principle, very costly 6D quadratures. Thus, if we are not interested in very accurate results, but only in semi-quantitative estimations of covalent energies, any procedure that might approximate the V_{xc} values in terms of cheaper to compute quantities like the DIs should be welcome. That procedure was initially examined by Rafat and Popelier,²⁷ being here extensively generalized.

Our expansion is based on writing V_{xc} as a multipolar series. We will show that the first (monopole-monopole) term is equal to that defined by Rafat and Popelier, and that the series is usually divergent although many times asymptotically convergent. Our results establish clearly in what conditions V_{xc} can be safely approximated by a truncated series, and that in some cases retaining up to the charge-quadrupole terms may give reasonable

results even for directly bonded atoms.

We will first consider the multipolar expansion of V_{xc} , including a short account of the IQA methodology. Then we will turn to examine how the series converges or diverges for a number of selected systems.

MULTIPOLAR EXPANSION OF V_{xc}^{AB}

In this section, we briefly describe the Interacting Quantum Atoms (IQA) method and the role played by the exchange-correlation (xc) interaction in this energy partition method (Subsection), the exact computation of this interaction (Subsection), and its multipolar approximation with or without truncating the expansion of the angular momentum series (Subsection 0.1). It is worth noting that the experience gained to date with the IQA method, both by us and by other groups, clearly indicates that the magnitude of V_{xc}^{AB} correlates very well with the degree of covalency between the pair of atoms A and B as measured by means of the delocalization index defined by Bader and Stephens, and weighted through the inverse of the distance between both atoms. As we will see, this correlation would be perfect as long as the crudest multipolar approximation to V_{xc}^{AB} (consisting in truncating the multipolar series in the term $l_1 = m_1 = l_2 = m_2 = 0$) were exact.

The Interacting Quantum Atoms (IQA) method

The IQA method^{4,5} is a real space energetic partition inspired in the Quantum Theory of Atoms in Molecules (QTAIM) that focuses on domain-averaged integrated quantities. The total energy in this approach is given by

$$E = \sum_A T_A + V_{en}^{AA} + V_{ee}^{AA} + \sum_{A>B} V_{nn}^{AB} + V_{en}^{AB} + V_{en}^{BA} + V_{ee}^{AB} \quad (1)$$

$$= \sum_A E_{self}^A + \sum_{A>B} E_{int}^{AB}. \quad (2)$$

where A runs over all the atoms in the molecule, $V_{nn}^{AB} = Z^A Z^B / R_{AB}$ is the repulsion between the nuclei A and B , $V_{en}^{AB} = -Z^B \int_{\Omega_A} d\mathbf{r}_1 \rho(\mathbf{r}_1) \mathbf{r}_{1B}^{-1}$ is the nuclear attraction of the electrons within the basin of A (Ω_A) to the nucleus B , and V_{ee}^{AB} is the total electron repulsion between

Ω_A and Ω_B . The latter is given by $V_{\text{ee}}^{\text{AB}} = J^{\text{AB}} + V_{\text{xc}}^{\text{AB}}$ where

$$J^{\text{AB}} = \int_{\Omega_A} d\mathbf{r}_1 \int_{\Omega_B} d\mathbf{r}_2 r_{12}^{-1} \rho(\mathbf{r}_1) \rho(\mathbf{r}_2), \quad (3)$$

is the classical or Coulomb electron-electrons repulsion, and

$$V_{\text{xc}}^{\text{AB}} = \int_{\Omega_A} d\mathbf{r}_1 \int_{\Omega_B} d\mathbf{r}_2 r_{12}^{-1} \rho_{\text{xc}}(\mathbf{r}_1, \mathbf{r}_2), \quad (4)$$

where $\rho_{\text{xc}}(\mathbf{r}_1, \mathbf{r}_2)$ is the exchange-correlation (xc) density, is the purely quantum-mechanical electron-electron xc interaction, which is the main subject of this work. In this way,

$$E_{\text{int}}^{\text{AB}} = (V_{\text{nn}}^{\text{AB}} + V_{\text{en}}^{\text{AB}} + V_{\text{en}}^{\text{BA}} + J^{\text{AB}}) + V_{\text{xc}}^{\text{AB}} = V_{\text{cl}}^{\text{AB}} + V_{\text{xc}}^{\text{AB}}. \quad (5)$$

The term $E_{\text{self}}^{\text{A}}$ in Eq. 2 collects all the energetic components affecting exclusively to the atom A while $E_{\text{int}}^{\text{AB}}$ represents the full interaction energy between atoms A and B , that is made of the full electrostatic or classical interaction ($V_{\text{cl}}^{\text{AB}}$) and the quantum-mechanical part ($V_{\text{xc}}^{\text{AB}}$). The expression 2 is valid, not only for the IQA methodology, but also for other energetic partitions, such as a recently proposed one inspired in the IQA method, although using a fuzzy partition of the space and localized molecular orbitals (MO).²⁸

The exact xc interaction energy

Over the years, it has become clear that the magnitude of $V_{\text{xc}}^{\text{AB}}$ measures the degree of covalency of the chemical bond between the atoms A and B . The more negative its value, the bigger the bond order between the two atoms and vice versa^{6,14,18}. Their values have been recently proposed as a novel solution to the problem of assigning a molecular graph to a collection of nuclei²³(i.e. how to draw a molecular structure). In the IQA approach, this term is exactly computed as follows. First, we use the fact that for both single- (1-det) and multi-determinant wavefunctions built in with real MOs ϕ_i , $\rho_{\text{xc}}(\mathbf{r}_1, \mathbf{r}_2)$ can be written as

$$\rho_{\text{xc}}(\mathbf{r}_1, \mathbf{r}_2) = \sum_{i,j,k,l}^M \lambda_{ijkl} \phi_i(\mathbf{r}_1) \phi_j(\mathbf{r}_1) \phi_k(\mathbf{r}_2) \phi_l(\mathbf{r}_2), \quad (6)$$

where M is the number of partially or fully occupied MOs, and λ_{ijkl} is a symmetric matrix in the (i, j) and (k, l) pairs. Defining a set of coefficients,

$$\epsilon_{ijkl} = \lambda_{ijkl} + \lambda_{jikl}(1 - \delta_{ij}) + \lambda_{ijlk}(1 - \delta_{kl}) + \lambda_{jilk}(1 - \delta_{ij})(1 - \delta_{kl}), \quad (7)$$

where δ_{ij} is the Kronecker symbol ($\delta_{ij} = 1$ for $i = j$, $\delta_{ij} = 0$ for $i \neq j$) we may write an $(i, j), (k, l)$ symmetric simpler expression,

$$\rho_{xc}(\mathbf{r}_1, \mathbf{r}_2) = \sum_{i \geq j, k \geq l}^M \epsilon_{ijkl} \phi_i(\mathbf{r}_1) \phi_j(\mathbf{r}_1) \phi_k(\mathbf{r}_2) \phi_l(\mathbf{r}_2). \quad (8)$$

Using the basis of products of MOs, $\{\phi_i(\mathbf{r})\phi_j(\mathbf{r}), i \geq j\}$, that contains $M(M+1)/2$ members, we diagonalize Eq. 8, and get:²⁹

$$\rho_{xc}(\mathbf{r}_1, \mathbf{r}_2) = \sum_{i \geq j}^M \eta_{ij} f_{ij}(\mathbf{r}_1) f_{ij}(\mathbf{r}_2), \quad (9)$$

where the f_{ij} eigenfunctions are linear combinations of the above products. The ϵ matrix may be easily computed from the explicit form of a given calculated wavefunction. For closed-shell 1-det wavefunctions (and formally also for a Kohn-Sham determinant) $M = N/2$, where N is the number of electrons, the ϵ matrix is already diagonal in the (i, j) and (k, l) pairs, each eigenvector is the product of two MOs, $f_{ij} = \phi_i \phi_j$, and the η_{ij} eigenvalues are simply $\eta_{ii} = -2$ and $\eta_{ij} = -4$ ($i \neq j$). Using Eq. 9 in the expression of V_{xc}^{AB} one gets

$$V_{xc}^{AB} = \sum_{i \geq j}^M \eta_{ij} K_{ij}^{AB}, \quad \text{where} \quad (10)$$

$$K_{ij}^{AB} = \int_{\Omega_A} d\mathbf{r}_1 \int_{\Omega_B} d\mathbf{r}_2 r_{12}^{-1} f_{ij}(\mathbf{r}_1) f_{ij}(\mathbf{r}_2). \quad (11)$$

The integrals 3 and 11 can be computed numerically and (in principle) exactly, i.e without invoking any approximation such as the multipolar expansion, by means of the bipolar expansion as described in Ref. 30.

0.1 The multipolar approach for V_{xc}^{AB}

Comparing Eq. 11 with Eq. 3 for the Coulomb repulsion it is evident that if J^{AB} is approximated making use of physically reasonable arguments that are also valid for K_{ij}^{AB} , the steps to approximate the latter will be the same used for J^{AB} . The long-range or multipolar approximation (MP) to J^{AB} , given by

$$J_{lr}^{AB} = \sum_{l_1 m_1}^{\infty} \sum_{l_2 m_2}^{\infty} C_{l_1 m_1 l_2 m_2}(\hat{R}) \frac{Q_{l_1 m_1}^{\Omega_A} Q_{l_2 m_2}^{\Omega_B}}{R^{l_1 + l_2 + 1}}, \quad (12)$$

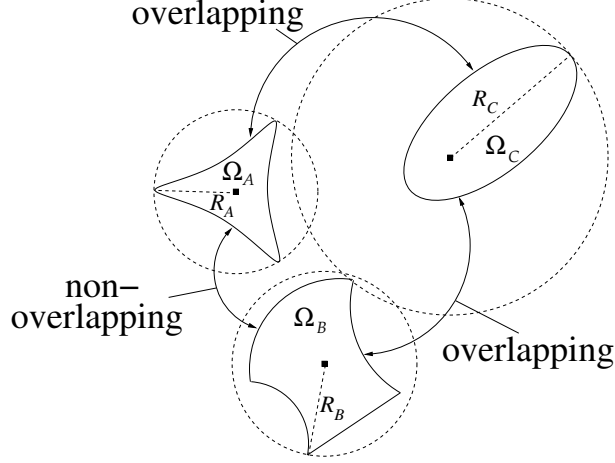


Figure 1: Schematic representation of overlapping and non-overlapping regions.

where m_1 (m_2) runs from $-l_1$ ($-l_2$) to $+l_1$ ($+l_2$), $\mathbf{R} = (\mathbf{R}_B - \mathbf{R}_A) \equiv (R, \hat{R})$ is the vector position of the B center with respect to the A center, $C_{l_1 m_1 l_2 m_2}(\hat{R})$ are known coefficients, Q_{lm}^Ω are the spherical atomic multipoles, defined as

$$Q_{lm}^\Omega = N_l \int_{\Omega} r^l S_{lm}(\hat{r}) \rho(\mathbf{r}) d\mathbf{r}, \quad (13)$$

$N_l = \sqrt{4\pi/(2l+1)}$, and $S_{lm}(\hat{r})$ are real spherical harmonics (see Appendix) is exact when the basins Ω_A and Ω_B are non-overlapping (See Fig. 1 and the definition of overlapping and non-overlapping regions below). Retaining only terms with $l_1 \leq 1$ and $l_2 \leq 1$ in Eq. 12 one has

$$J_{\text{lr,cd}}^{\text{AB}} \simeq \frac{Q^A Q^B}{R} - Q^A \frac{\vec{\mu}^B \cdot \mathbf{R}}{R^3} + Q^B \frac{\vec{\mu}^A \cdot \mathbf{R}}{R^3} + \frac{1}{R^3} \left(\vec{\mu}^A \cdot \vec{\mu}^B - 3 \frac{(\vec{\mu}^A \cdot \mathbf{R})(\mathbf{R} \cdot \vec{\mu}^B)}{R^2} \right), \quad (14)$$

where $Q^\Omega = \int_{\Omega} \rho(\mathbf{r}) d\mathbf{r}$ and $\vec{\mu}^\Omega = \int_{\Omega} \mathbf{r} \rho(\mathbf{r}) d\mathbf{r}$ are the total electron charge and the dipole moment of the Ω region, respectively. The first, second plus third, and fourth terms of 14 correspond to the charge-charge (cc), charge-dipole (cd), and dipole-dipole (dd) interactions, respectively. We should note that the second and third terms have opposite signs.

If the same approximation is used for K_{ij}^{AB} , $(V_{xc}^{AB})_{lr}$ becomes

$$(V_{xc}^{AB})_{lr} = \sum_{l_1 m_1}^{\infty} \sum_{l_2 m_2}^{\infty} C_{l_1 m_1 l_2 m_2}(\hat{R}) \frac{\delta_{l_1 m_1, l_2 m_2}^{AB}}{R^{l_1 + l_2 + 1}}, \quad \text{where} \quad (15)$$

$$\delta_{l_1 m_1, l_2 m_2}^{AB} = \sum_{i \geq j}^M \eta_{ij} q_{ij, l_1 m_1}^{\Omega_A} q_{ij, l_2 m_2}^{\Omega_B}, \quad \text{and} \quad (16)$$

$$q_{ij, lm}^{\Omega} = N_l \int_{\Omega} r^l S_{lm}(\hat{r}) f_{ij}(\mathbf{r}) d\mathbf{r}. \quad (17)$$

It is important to stress that, similarly to $(J^{AB})_{lr}$, the expression 15 for $(V_{xc}^{AB})_{lr}$ provides the exact xc interaction when the atomic basins Ω_A and Ω_B do not overlap (Fig. 1). In the present context these two basins are non-overlapping because the two spheres of radii R_A and R_B , centered at the origin of Ω_A and Ω_B , respectively, do not intersect each other, being R_A (R_B) the maximum distance from the origin of the basin to the surface of Ω_A (Ω_B). On the contrary, Ω_A and Ω_C are overlapping despite that none point inside Ω_A belongs also to Ω_C and viceversa. When the non-overlapping condition is not met, the current expressions for $(J^{AB})_{lr}$ and $(V_{xc}^{AB})_{lr}$ are only conditionally convergent. We will see different examples of this in Section 0.1.

The function $N_l r^l S_{lm}(\hat{r})$ is 1 for $l = m = 0$, (y, z, x) for $l = 1$ and $m = (-1, 0, +1)$, and $(\sqrt{3}xy, \sqrt{3}yz, \frac{1}{2}(3z^2 - r^2), \sqrt{3}xz, \frac{\sqrt{3}}{2}(x^2 - y^2))$ for $l = 2$ and $m = (-2, -1, 0, +1, +2)$. If, as in the case of J^{AB} , only terms with $l_1 \leq 1$ and $l_2 \leq 1$ are included, $(V_{xc}^{AB})_{lr}$ becomes

$$(V_{xc}^{AB})_{lr, cd} \simeq \sum_{i, j} \eta_{ij} \left[\frac{q_{ij}^{\Omega_A} q_{ij}^{\Omega_B}}{R} - q_{ij}^{\Omega_A} \frac{\vec{\mu}_{ij}^{\Omega_B} \cdot \mathbf{R}}{R^3} + q_{ij}^{\Omega_B} \frac{\vec{\mu}_{ij}^{\Omega_A} \cdot \mathbf{R}}{R^3} + \frac{1}{R^3} \left(\vec{\mu}_{ij}^{\Omega_A} \cdot \vec{\mu}_{ij}^{\Omega_B} - 3 \frac{(\vec{\mu}_{ij}^{\Omega_A} \cdot \mathbf{R})(\mathbf{R} \cdot \vec{\mu}_{ij}^{\Omega_B})}{R^2} \right) \right], \quad (18)$$

where $q_{ij}^{\Omega} \equiv q_{ij, 00}^{\Omega} = \int_{\Omega} f_{ij}(\mathbf{r}) d\mathbf{r}$, and

$$\vec{\mu}_{ij}^{\Omega} \equiv (q_{ij, 1-1}^{\Omega}, q_{ij, 10}^{\Omega}, q_{ij, 1+1}^{\Omega}) = \int_{\Omega} \mathbf{r} f_{ij}(\mathbf{r}) d\mathbf{r}. \quad (19)$$

If terms with $(l_1 = 0, l_2 = 2)$ and $(l_1 = 2, l_2 = 0)$ are also included, the extra contribution

$$(V_{xc}^{AB})_{lr, cq} = \sum_{i, j} \frac{\eta_{ij}}{R^3} \sum_{m=-2}^{+2} q_{2m}(\hat{R}) [q_{ij}^A q_{ij, 2m}^B + q_{ij}^B q_{ij, 2m}^A] \quad (20)$$

must be added to 18. The *cq* subscript in Eq. 20 stands for *charge-quadrupole* interactions. The improved expression for $(V_{xc}^{AB})_{lr}$ is then

$$(V_{xc}^{AB})_{lr,cdq} = (V_{xc}^{AB})_{lr,cd} + (V_{xc}^{AB})_{lr,cq}. \quad (21)$$

The physical meaning of q_{ij}^Ω and $\vec{\mu}_{ij}^\Omega$ are easy to grasp. If we consider the particular case of their diagonal expressions ($i = j$) for a 1-det wavefunction, $f_{ii}(\mathbf{r}) = \phi_i^2(\mathbf{r})$, so that q_{ii}^Ω is the electron charge of the orbital distribution $\phi_i^2(\mathbf{r})$ within the Ω region, and $\vec{\mu}_{ii}^\Omega$ the dipole moment of Ω due to this distribution. For this reason, q_{ij}^Ω and $\vec{\mu}_{ij}^\Omega$ may be called orbital overlap charge and orbital overlap dipole, respectively. At the Hartree-Fock (HF) level, the q_{ij}^Ω 's coincide with the Atomic Overlap Matrix (AOM) elements of the QTAIM, $q_{ij}^\Omega \equiv \langle \phi_i | \phi_j \rangle_\Omega = S_{ij}^\Omega$. However, given that $f_{ij}(\mathbf{r})$ at the correlated level is a linear combination of $\phi_i(\mathbf{r})\phi_j(\mathbf{r})$ products, q_{ij}^Ω in this case is a linear combination of AOM elements. Nevertheless, for both types of wavefunctions $-2\delta_{00,00}^{AB}$ coincides with δ^{AB} , the so-called delocalization index (DI) between the atoms A and B

$$-2\delta_{00,00}^{AB} = \delta^{AB} = - \sum_{i \geq j}^M 2\eta_{ij} S_{ij}^{\Omega_A} S_{ij}^{\Omega_B}, \quad (22)$$

so that the leading term of $(V_{xc}^{AB})_{lr}$ ($l_1 = l_2 = m_1 = m_2 = 0$) can be written as

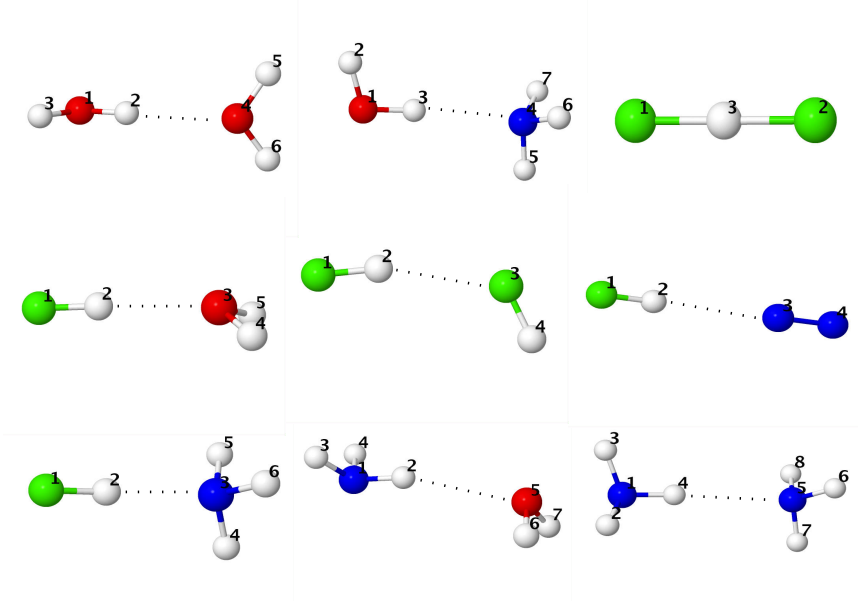
$$R^{-1} \sum_{i,j} \eta_{ij} q_{ij}^{\Omega_A} q_{ij}^{\Omega_B} = -\delta^{AB} / (2R). \quad (23)$$

The above equation is behind the good existing correlation between the values of V_{xc}^{AB} and δ^{AB} for a large collection of AB couples in many systems. The present derivation shows that the proportionality between V_{xc}^{AB} and δ^{AB} is modulated by the inverse of the distance between the nuclei of both atomic basins.

SYSTEMS AND COMPUTATIONAL DETAILS

All the calculations of this work have performed with our PROMOLDEN code.³¹ This program allows the exact computation^{29,30} (i.e., without suffering the convergence problems inherent to the multipolar series expansion) of V_{xc}^{AB} as well as the full (lr) and truncated (lr,cd) and (lr,cdq) multipolar approximations described in Section . For brevity, only the exact,

Figure 2: Hydrogen bond systems studied in this work. Hydrogen, nitrogen, oxygen, and fluorine atoms are represented in white, blue, red, and green, respectively.

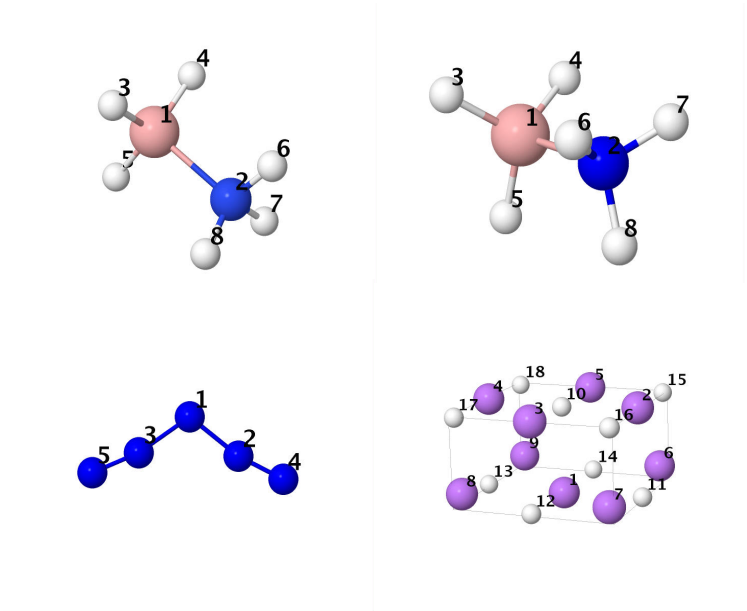


and the (lr) and (lr,cdq) numbers will be given in the tables. The errors plotted in the figures are defined as $[(V_{xc}^{AB})_{\text{method}} - (V_{xc,\text{exact}}^{AB})]/|V_{xc,\text{exact}}^{AB}| \times 100$, where method = (lr), (lr,cd), or (lr,cdq). The studied systems include several standard hydrogen bonded (HB) dimers (Fig. 2), the staggered BH_3NH_3 , eclipsed BH_3NH_3 , N_5^+ , and Li_9H_9 molecules (Fig 3), eleven molecules derived from saturated hydrocarbons by substituting C or H atoms by Be, B, N, O, F atoms, plus the benzene molecule (Fig. 4), the saturated hydrocarbons ethane, propane, butane, and pentane (Fig. 5), and the phenol dimer (Fig. 6). The labels of the atoms in the tables are those defined in these figures. For simplicity, the molecular orbitals required for evaluating the exchange-correlation density of Eq. 8 have been obtained through restricted Hartree-Fock (RHF) calculations at the corresponding equilibrium geometries with basis sets of quality 6-311G(d,p) or higher. We do not expect, however, significant changes neither in the numerical results nor in the subsequent discussion when using more accurate wavefunctions or Kohn-Sham determinants in the computation of the xc interactions. Since the calculations are RHF, the V_{xc}^{AB} energies lack of the correlation energy component and should be more properly called V_x^{AB} . However, since all the expressions in Section are valid for general wavefunctions the original name will be used hereinafter.

Table 1: xc interaction energies ≥ 0.1 kJ/mol for the HB dimers of Fig. 2.

$A - B$	$(V_{xc}^{AB})_{lr,cdq}$	$(V_{xc}^{AB})_{lr}$	V_{xc}^{AB}	$A - B$	$(V_{xc}^{AB})_{lr,cdq}$	$(V_{xc}^{AB})_{lr}$	V_{xc}^{AB}
H₂O–H₂O				HF–NH₃			
O ₁ –H ₂	-478.59	1.29×10^4	-437.77	F ₁ –H ₂	-280.40	3.79×10^3	-259.76
O ₁ –H ₃	-569.61	-8.45×10^5	-514.46	F ₁ –N ₃	-40.44	-41.74	-41.85
O ₁ –O ₄	-16.40	-16.96	-16.94	F ₁ –H ₄	-0.42	-0.42	-0.42
O ₁ –H ₅	-0.11	-0.10	-0.11	F ₁ –H ₅	-0.42	-0.42	-0.42
H ₂ –H ₃	-1.94	-1.44	-1.84	F ₁ –H ₆	-0.42	-0.42	-0.42
H ₂ –O ₄	-24.73	-25.45	-25.36	H ₂ –N ₃	-47.99	-48.50	-48.23
H ₂ –H ₅	-0.17	-0.17	-0.17	H ₂ –H ₄	-0.34	-0.34	-0.34
H ₃ –O ₄	-0.19	-0.18	-0.18	H ₂ –H ₅	-0.34	-0.34	-0.34
O ₄ –H ₅	-541.14	-7.16×10^5	-488.52	H ₂ –H ₆	-0.34	-0.34	-0.34
H ₅ –H ₆	-2.19	-4.27	-2.03	N ₃ –H ₄	-758.46	5.38×10^5	-688.30
H₂O–NH₃				N ₃ –H ₅	-758.46	5.38×10^5	-688.30
O ₁ –H ₂	-575.13	-1.21×10^7	-519.23	N ₃ –H ₆	-758.40	5.58×10^5	-688.24
O ₁ –H ₃	-460.75	-5.35×10^4	-421.84	H ₄ –H ₅	-5.34	-12.72	-5.12
O ₁ –N ₄	-20.16	-20.71	-20.70	H ₄ –H ₆	-5.34	-12.71	-5.12
O ₁ –H ₅	-0.19	-0.19	-0.19	H ₅ –H ₆	-5.34	-12.71	-5.12
O ₁ –H ₆	-0.20	-0.20	-0.20	NH₃–H₂O			
H ₂ –H ₃	-1.88	-1.00	-1.80	N ₁ –H ₂	-731.84	4.54×10^6	-668.43
H ₂ –N ₄	-0.24	-0.24	-0.24	N ₁ –H ₃	-779.59	1.37×10^6	-710.26
H ₃ –N ₄	-31.54	-32.23	-32.07	N ₁ –O ₅	-8.33	-8.63	-8.60
H ₃ –H ₅	-0.27	-0.27	-0.27	H ₂ –H ₃	-5.26	-6.18	-5.13
H ₃ –H ₆	-0.28	-0.28	-0.28	H ₂ –O ₅	-16.83	-17.59	-17.37
N ₄ –H ₅	-764.79	6.93×10^5	-694.12	H ₂ –H ₆	-0.10	-0.10	-0.10
N ₄ –H ₆	-767.36	5.65×10^5	-697.06	H ₃ –H ₄	-6.08	-30.52	-5.85
H ₅ –H ₆	-5.60	-17.52	-5.37	H ₃ –O ₅	-0.20	-0.20	-0.20
H ₆ –H ₇	-5.66	-18.08	-5.43	O ₅ –H ₆	-550.78	-8.08×10^5	-496.97
FHF⁻				H ₆ –H ₇	-2.27	-4.67	-2.11
F ₁ –F ₂	-92.79	-100.02	-96.55	NH₃–NH₃			
F ₁ –H ₃	-163.82	6.80×10^4	-159.19	N ₁ –H ₂	-781.96	7.75×10^5	-712.71
HF–H₂O				N ₁ –H ₄	-719.70	-1.22×10^5	-657.38
F ₁ –H ₂	-298.63	-844.89	-275.72	N ₁ –N ₅	-9.02	-9.29	-9.26
F ₁ –O ₃	-28.64	-29.82	-29.79	H ₂ –H ₃	-6.16	-35.32	-5.93
F ₁ –H ₄	-0.23	-0.22	-0.22	H ₂ –H ₄	-5.16	1.88	-5.04
H ₂ –O ₃	-32.04	-32.78	-32.67	H ₂ –N ₅	-0.22	-0.22	-0.22
H ₂ –H ₄	-0.23	-0.23	-0.23	H ₄ –N ₅	-20.79	-21.40	-21.28
O ₃ –H ₄	-528.95	-5.93×10^5	-477.77	H ₄ –H ₆	-0.24	-0.24	-0.24
H ₄ –H ₅	-2.11	-4.02	-1.96	H ₄ –H ₇	-0.20	-0.20	-0.20
HF–HF				N ₅ –H ₆	-771.52	7.64×10^5	-702.05
F ₁ –H ₂	-329.20	7048.78	-302.00	N ₅ –H ₇	-770.75	6.85×10^5	-700.44
F ₁ –F ₃	-17.02	-17.83	-17.82	H ₆ –H ₇	-5.80	-22.66	-5.57
H ₂ –F ₃	-16.71	-17.34	-17.32	H ₇ –H ₈	-5.75	-21.54	-5.52
H ₂ –H ₄	-0.11	-0.11	-0.11	HF–N₂			
F ₃ –H ₄	-356.83	-2.05×10^5	-320.36	F ₁ –H ₂	-349.90	-5.85×10^3	-319.67
HF–N₂				F ₁ –N ₃	-9.19	-9.58	-9.57
F ₁ –H ₂	-349.90	-5.85×10^3	-319.67	F ₁ –N ₄	-0.28	-0.28	-0.28
F ₁ –N ₃	-9.19	-9.58	-9.57	H ₂ –N ₃	-11.15	-11.46	-11.46
F ₁ –N ₄	-0.28	-0.28	-0.28	H ₂ –N ₄	-0.46	-0.45	-0.45
H ₂ –N ₃	-11.15	-11.46	-11.46	N ₃ –N ₄	-2266.80	-8.61×10^5	-2479.99
H ₂ –N ₄	-0.46	-0.45	-0.45				
N ₃ –N ₄	-2266.80	-8.61×10^5	-2479.99				

Figure 3: Staggered BH_3NH_3 , eclipsed BH_3NH_3 , N_5^+ , and Li_9H_9 molecules. Hydrogen, lithium, boron, and nitrogen atoms are represented in white, indigo, pink, and blue, respectively.



RESULTS AND DISCUSSION

The more representative results regarding the approximate V_{xc}^{AB} values, as well as their errors for the systems listed in Section 0.1 are gathered in Tables 1-4 and Figs. 7-11. We can see in Table 1, where the V_{xc}^{AB} 's for the HB systems of Fig. 2 are collected, that the full multipolar approximation $(V_{xc}^{AB})_{lr}$ (Eq. 15) fails miserably for all intramolecular A–H pairs ($A=\text{N},\text{O},\text{F}$). Surprisingly, the crude (lr,cdq) approximation gives xc interactions with relative errors of about 10% or smaller for the intramolecular directly bonded atoms. Regarding the intermolecular interactions, the xc energy between the two atoms involved in the HB is well represented by $(V_{xc}^{AB})_{lr}$, with differences with respect to the exact values smaller than 0.3 kJ/mol in all the cases. We note again that the (lr,cdq) values differ only by 0.3-0.6 kJ/mol from the exact ones, confirming that the multipolar expansion for these interactions is practically converged at this level of calculation. Intermolecular A–H and H–H xc energies other than the above ones are given by the lr approximation with errors smaller than 0.1 and 0.01 kJ/mol, respectively. For the intermolecular H–H energies, the same is true in the (lr,cdq) approximation. However, the xc interaction between the A atom of the protor

Figure 4: Molecules derived from saturated hydrocarbons by substituting C or H atoms by Be, B, N, O, F atoms, plus the benzene molecule. Hydrogen, lithium, beryllium, boron, carbon, nitrogen, oxygen, and fluorine atoms are represented in white, indigo, gold, pink, grey, blue, red, and green, respectively.

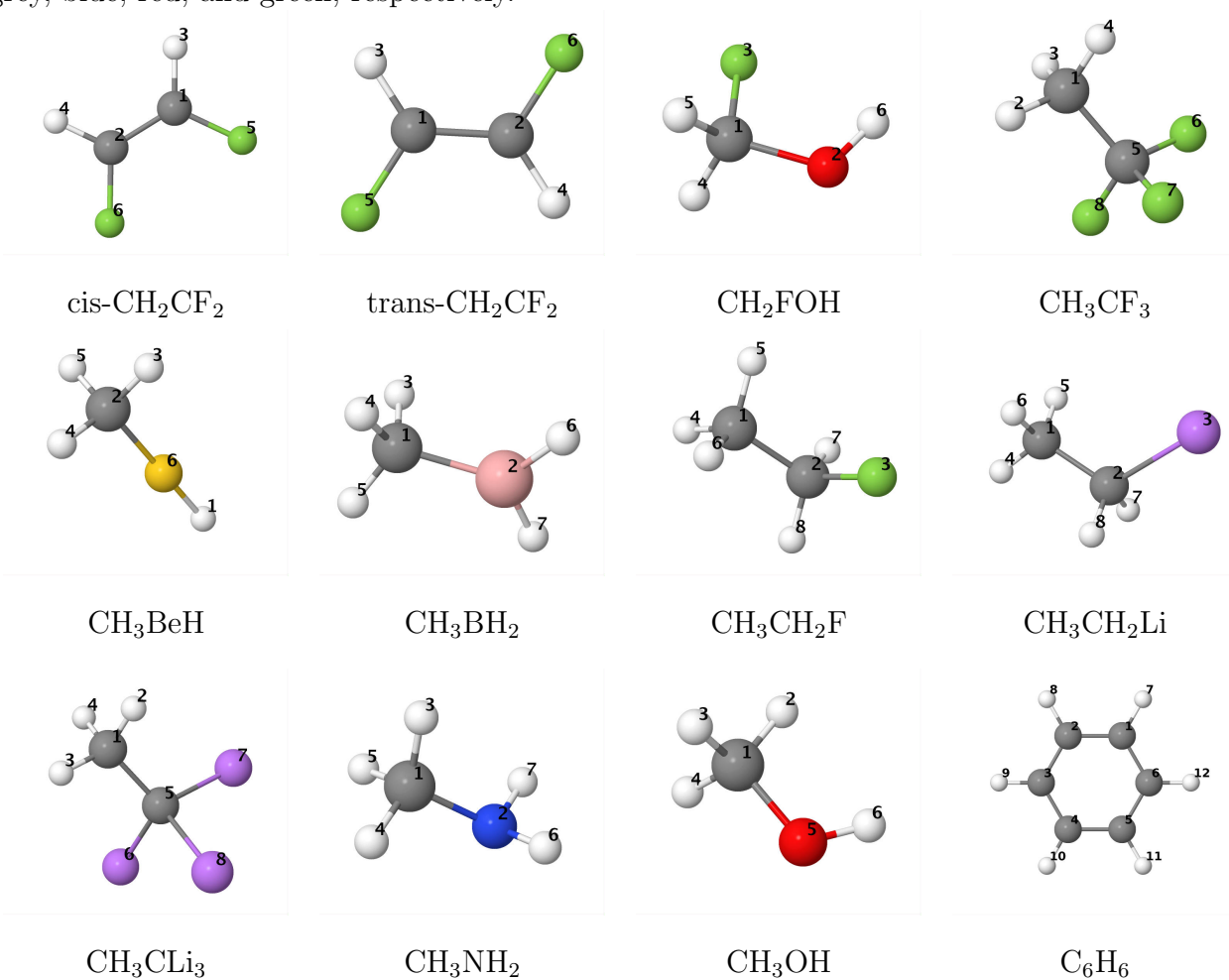


Figure 5: C_nH_{2n+2} ($n = 2 - 5$) saturated hydrocarbons.

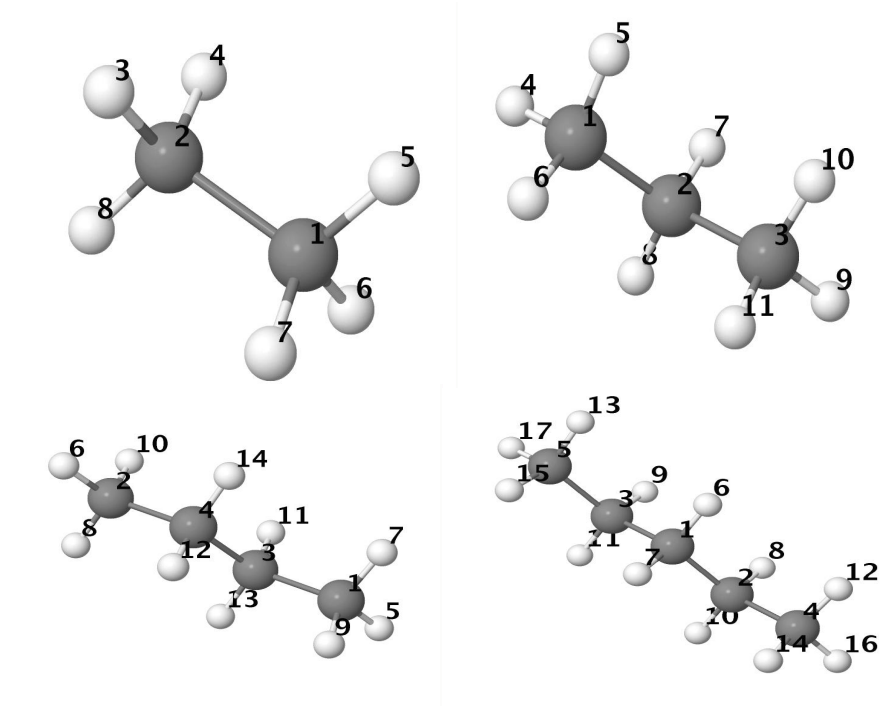
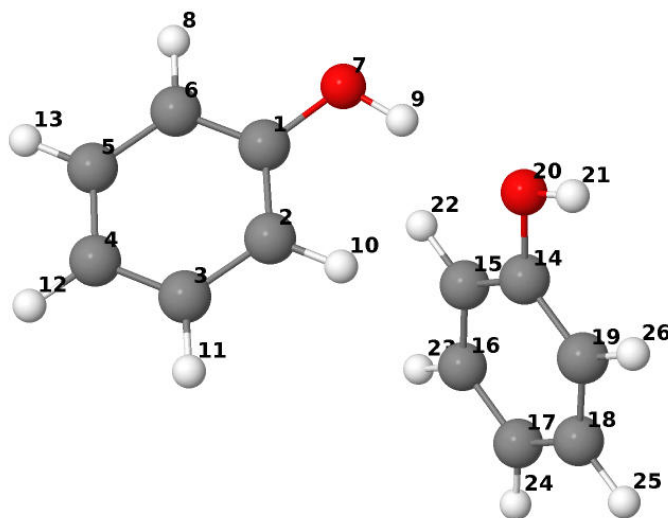


Figure 6: Phenol dimer.



donor (PD) and the B atom of the proton acceptor (PA) molecule is predicted with errors as large as 1.4 kJ/mol ($\text{FH}\cdots\text{NH}_3$) when the (lr,cdq) approximation is used, which clearly indicates that multipolar interactions higher than the charge-quadrupole ones included in this approximation are required to represent this type of interaction with accuracy.

The relative errors of the A–B, A–H (A,B=N,O,F), and H–H xc interaction energies for all the intra and intermolecular pairs of the HB systems are represented in Fig. 7. We observe in Fig. 7 that cd and cdq intramolecular H–H energies are, in general, more accurate than A–H interactions, which is clearly due to the 1–3 (1–2) character of all the intramolecular H–H (A–H) pairs. It is also striking that, with a couple of exceptions, cdq relative errors are negative whereas the contrary happens with the cd approximation. Moreover, as previously commented, only a single lr relative error appears in the figure, the remaining ones having errors greater than 20%. Regarding the intermolecular xc energies we observe in right Fig. 7 the progressive decreasing of relative errors in passing from cd to cdq, and from cdq to lr.

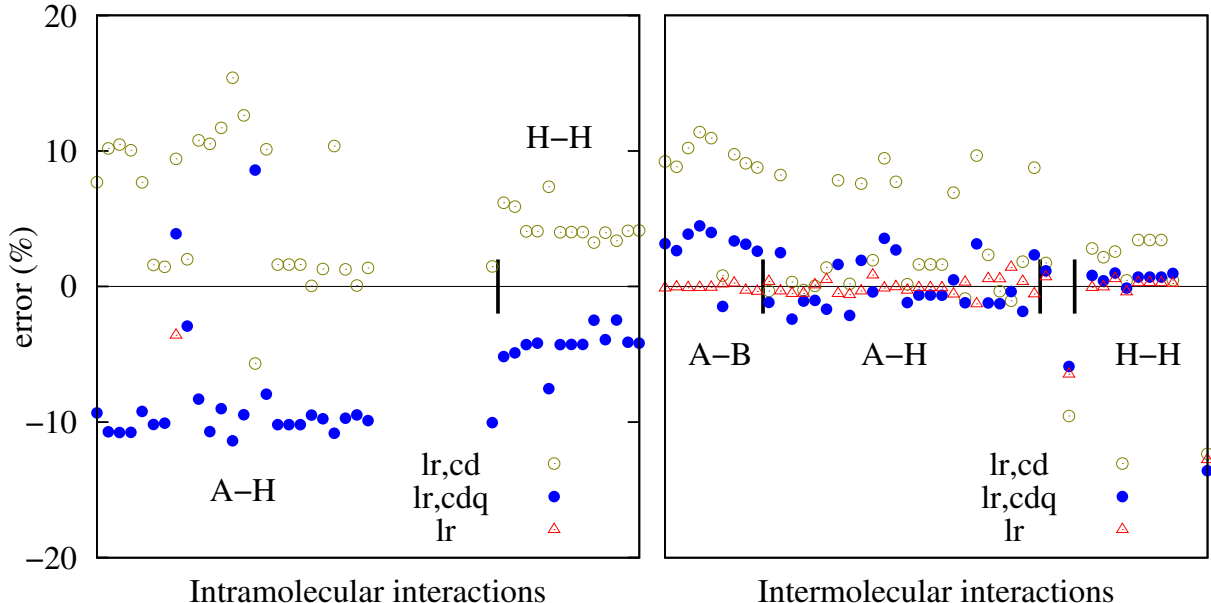
The discussion for the systems in Fig. 3 runs parallel to that of the HB dimers. The $(V_{xc}^{AB})_{lr}$ value for the B–N pair in eclipsed and staggered $\text{BH}_3\text{--NH}_3$ has no sense. Similarly, the lr xc interaction between the directly bonded (i.e. 1–2) B–H and N–H pairs is quite absurd. Not only that, but also the $(V_{xc}^{AB})_{lr}$'s for the 1–3 pairs $\text{H}_3\text{--H}_4$ and $\text{H}_6\text{--H}_7$ are several orders of magnitude greater than the exact values. Contrarily to this, the cdq approximation works relatively well for the B–N pair and the 1–2 B–H and N–H pairs (relative error < 5%). The $\text{H}_3\text{--H}_4$ interaction is also extremely well reproduced by this approximation (error < 0.2%), whereas the $\text{H}_6\text{--H}_7$ is slightly worse (error \sim 4%). The xc interaction between the B atom and a H atom of the NH_3 unit ($\text{B}_1\text{--H}_6$) is fairly accurate in both the lr and cdq approximations. This is not so with the symmetric interaction $\text{N}_2\text{--H}_3$, with errors about 4–7% in both cases.

In the N_5^+ molecule, the xc energy for the 1–2 pairs is again badly represented by the lr approximation but is reasonable in the cdq approach, particularly for $\text{N}_1\text{--N}_2$. The cdq and lr values for the 1–3 $\text{N}_1\text{--N}_4$ interaction differs from the exact value by about 0.9 and 0.3 kJ/mol, respectively. The error in the other 1–3 interaction ($\text{N}_2\text{--N}_3$) is considerably higher in both approaches. Finally, the lr and cdq xc energies for the 1–4 $\text{N}_2\text{--N}_5$ and 1–5 $\text{N}_4\text{--N}_5$ pairs are practically the same and coincident with the exact value. This result highlights

Table 2: Representative xc interaction energies (kJ/mol) for the systems of Fig. 3. In Li_9H_9 the directly bonded Li and H atoms are signalled with (1).

$A - B$	$(V_{xc}^{AB})_{\text{lr,cdq}}$	$(V_{xc}^{AB})_{\text{lr}}$	V_{xc}^{AB}	$A - B$	$(V_{xc}^{AB})_{\text{lr,cdq}}$	$(V_{xc}^{AB})_{\text{lr}}$	V_{xc}^{AB}
eclipsed $\text{BH}_3\text{-NH}_3$				Li_9H_9			
$\text{B}_1\text{-N}_2$	-164.57	3524.65	-172.41	$\text{Li}_1\text{-Li}_2$	-0.30	-0.31	-0.31
$\text{B}_1\text{-H}_3$	-355.03	8.40×10^6	-334.69	$\text{Li}_1\text{-Li}_6$	-0.71	-0.72	-0.72
$\text{B}_1\text{-H}_6$	-1.15	-1.14	-1.14	$\text{Li}_1\text{-H}_{10}(1)$	-17.22	-318.57	-17.75
$\text{N}_2\text{-H}_3$	-60.32	-62.95	-65.25	$\text{Li}_1\text{-H}_{11}(1)$	-25.92	42.71	-26.24
$\text{N}_2\text{-H}_6$	-723.06	-8.05×10^7	-659.17	$\text{Li}_1\text{-H}_{15}$	-0.47	-0.49	-0.49
$\text{H}_3\text{-H}_4$	-67.52	-339.26	-67.39	$\text{Li}_2\text{-Li}_3$	-0.70	-0.93	-0.71
$\text{H}_3\text{-H}_6$	-2.58	-4.71	-2.55	$\text{Li}_2\text{-Li}_4$	-0.14	-0.14	-0.14
$\text{H}_3\text{-H}_7$	-0.69	-0.68	-0.69	$\text{Li}_2\text{-Li}_6$	-0.84	-0.87	-0.85
$\text{H}_6\text{-H}_7$	-4.30	-865.54	-4.12	$\text{Li}_2\text{-H}_{10}(1)$	-26.95	331.98	-27.12
staggered $\text{BH}_3\text{-NH}_3$				$\text{Li}_2\text{-H}_{11}(1)$	-18.34	59.37	-18.74
$\text{B}_1\text{-N}_2$	-172.72	3080.97	-181.51	$\text{Li}_2\text{-H}_{12}$	-0.47	-0.50	-0.49
$\text{B}_1\text{-H}_3$	-351.06	7.76×10^6	-331.51	$\text{Li}_2\text{-H}_{13}$	-0.09	-0.10	-0.09
$\text{B}_1\text{-H}_6$	-1.21	-1.99	-1.20	$\text{Li}_2\text{-H}_{15}(1)$	-36.35	1.50×10^4	-36.27
$\text{N}_2\text{-H}_3$	-64.56	-71.22	-69.56	$\text{Li}_2\text{-H}_{17}$	-0.17	-0.17	-0.17
$\text{N}_2\text{-H}_6$	-721.25	-6.056×10^8	-659.38	$\text{Li}_6\text{-Li}_7$	-0.31	-0.31	-0.31
$\text{H}_3\text{-H}_4$	-66.25	-296.87	-66.17	$\text{Li}_6\text{-H}_{10}$	-0.84	-0.88	-0.88
$\text{H}_3\text{-H}_6$	-1.06	-1.17	-1.05	$\text{Li}_6\text{-H}_{11}(1)$	-36.95	36.59	-36.67
$\text{H}_3\text{-H}_7$	-1.62	-1.61	-1.61	$\text{Li}_6\text{-H}_{12}$	-0.19	-0.19	-0.19
$\text{H}_6\text{-H}_7$	-4.28	-472.57	-4.12	$\text{Li}_6\text{-H}_{15}(1)$	-45.11	-1.21×10^3	-44.54
N_5^+				$\text{Li}_6\text{-H}_{16}$	-0.21	-0.21	-0.21
$\text{N}_1\text{-N}_2$	-1019.33	-1.70×10^5	-1056.45	$\text{H}_{10}\text{-H}_{11}$	-18.30	-20.78	-19.85
$\text{N}_1\text{-N}_4$	-47.28	-48.48	-48.20	$\text{H}_{10}\text{-H}_{15}$	-29.91	-38.97	-30.92
$\text{N}_2\text{-N}_3$	-52.15	-62.35	-55.59	$\text{H}_{11}\text{-H}_{12}$	-24.03	-36.36	-24.76
$\text{N}_2\text{-N}_4$	-2066.45	2.90×10^7	-2205.41	$\text{H}_{11}\text{-H}_{13}$	-0.70	-0.71	-0.70
$\text{N}_2\text{-N}_5$	-7.78	-7.77	-7.77	$\text{H}_{11}\text{-H}_{15}$	-25.73	-49.73	-26.56
$\text{N}_4\text{-N}_5$	-3.26	-3.27	-3.27	$\text{H}_{11}\text{-H}_{17}$	-0.28	-0.28	-0.28
				$\text{H}_{15}\text{-H}_{16}$	-1.48	-1.47	-1.44
				$\text{H}_{15}\text{-H}_{17}$	-0.19	-0.19	-0.19

Figure 7: Relative errors, $[(V_{xc}^{AB})_{\text{method}} - (V_{xc,\text{exact}}^{AB})]/|V_{xc,\text{exact}}^{AB}| \times 100$, of the intra- (left) and intermolecular (right) interactions of the molecules in Fig. 2.



two important facts: i) the atomic basins of N_2 and N_5 (or N_4 and N_5) atoms fulfill almost exactly the non-overlapping criterion displayed in Fig. 1, and ii) the multipolar series 15 converges very quickly in this particular case.

Finally, the results for Li_9-H_9 reinforce what was said in the above three paragraphs. The full lr expansion fails completely in predicting xc interaction energies for 1–2 Li–H pairs, while the cdq values are pretty accurate. All Li–Li xc energies are well represented in the lr and cdq approximations, with the exception of the lr Li_2-Li_3 interaction. This is probably related with the almost spherical character of Li atomic basins. According to this, the 1–3 Li–H lr xc energies and, more importantly, the 1–3 H–H xc energies are less accurately computed due to the far from the spherical character of H atomic basins. This is exacerbated in the lr approximation, where higher angular number l values are involved (see Eq. 17).

The xc pair interaction energies of the systems in Fig. 4 are collected in Tables 3 and 4, and the relative errors of the cd, cdq and lr approximate values displayed in Fig. 8, for the 1–2 (left-top), 1–3 (right-top), and 1–4 (bottom) pairs, respectively. Virtually all of the above comments also apply here: the 1–2 xc interactions can not be represented at all

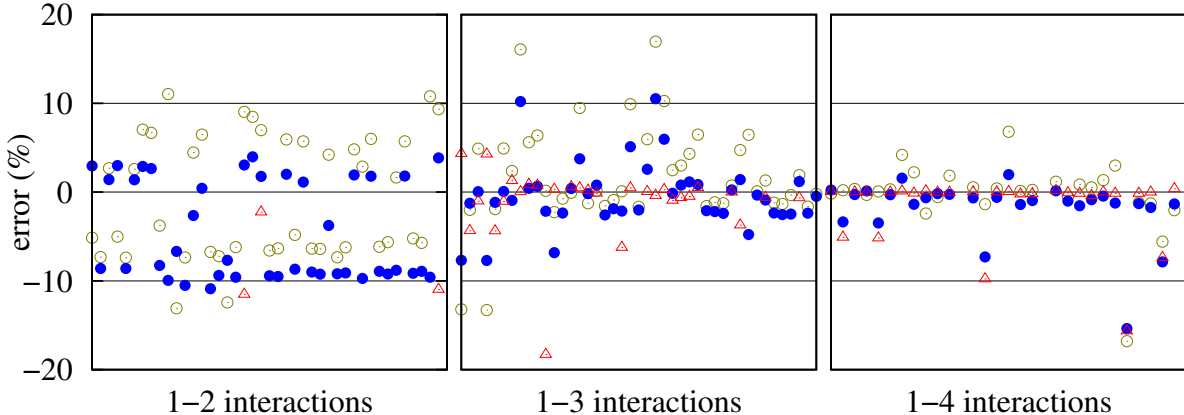
Table 3: Representative xc interaction energies (kJ/mol) for the systems of Fig. 4.

$A - B$	$(V_{xc}^{AB})_{lr,cdq}$	$(V_{xc}^{AB})_{lr}$	V_{xc}^{AB}	$A - B$	$(V_{xc}^{AB})_{lr,cdq}$	$(V_{xc}^{AB})_{lr}$	V_{xc}^{AB}
<i>cis</i>-C₂H₂F₂				CH₃BeH			
C ₁ -C ₂	-1311.48	-3.82×10 ⁵	-1351.45	H ₁ -C ₂	-34.84	-32.52	-32.62
C ₁ -H ₃	-811.14	-1.20×10 ⁴	-746.88	H ₁ -H ₃	-0.75	-0.74	-0.75
C ₁ -H ₄	-17.00	-15.11	-15.79	H ₁ -Be ₆	-170.49	2.43×10 ⁴	-159.81
C ₁ -F ₅	-600.29	-5.29×10 ³	-608.87	C ₂ -H ₃	-845.84	6.99×10 ⁵	-765.34
C ₁ -F ₆	-53.21	-54.86	-52.56	C ₂ -Be ₆	-168.87	-824.46	-164.53
H ₃ -H ₄	-1.40	-1.40	-1.40	H ₃ -H ₄	-17.84	-30.31	-17.43
H ₃ -F ₅	-24.53	-24.79	-24.54	H ₃ -Be ₆	-2.46	-2.45	-2.47
H ₃ -F ₆	-3.64	-3.70	-3.52	CH₃BH₂			
F ₅ -F ₆	-4.61	-4.60	-4.60	C ₁ -B ₂	-361.03	-496.34	-362.60
<i>trans</i>-C₂H₂F₂				C ₁ -H ₃	-826.73	2.48×10 ⁵	-745.50
C ₁ -C ₂	-1304.91	-3.87×10 ⁵	-1345.33	C ₁ -H ₄	-834.27	6.39×10 ⁴	-762.61
C ₁ -H ₃	-811.92	-540.92	-747.51	C ₁ -H ₆	-66.37	-68.63	-68.96
C ₁ -H ₄	-16.93	-15.04	-15.72	B ₂ -H ₃	-6.72	-6.70	-6.71
C ₁ -F ₅	-603.33	-5.67×10 ³	-611.80	B ₂ -H ₄	-4.08	-4.11	-4.11
C ₁ -F ₆	-54.31	-56.04	-53.69	B ₂ -H ₆	-376.42	-1.85×10 ⁴	-349.54
H ₃ -H ₄	-1.37	-1.38	-1.38	H ₃ -H ₄	-17.11	-25.73	-16.68
H ₃ -F ₅	-24.82	-25.10	-24.84	H ₃ -H ₆	-2.04	-2.04	-2.04
H ₃ -F ₆	-3.66	-3.72	-3.53	H ₄ -H ₅	-15.65	-21.75	-15.36
F ₅ -F ₆	-4.71	-4.69	-4.69	H ₄ -H ₆	-2.82	-2.81	-2.81
CH₂FOH				H ₄ -H ₇	-2.11	-2.10	-1.72
C ₁ -O ₂	-595.20	1.19×10 ³	-613.00	H ₆ -H ₇	-66.83	-69.51	-65.42
C ₁ -F ₃	-515.50	80.74	-529.59	CH₃CH₂F			
C ₁ -H ₄	-784.72	-1.93×10 ⁴	-724.78	C ₁ -C ₂	-776.25	-808.13	-790.31
C ₁ -H ₆	-3.15	-3.08	-3.12	C ₁ -F ₃	-34.45	-36.53	-36.63
O ₂ -F ₃	-84.54	-94.13	-94.16	C ₁ -H ₄	-818.55	5.40×10 ⁴	-748.07
O ₂ -H ₄	-29.48	-29.36	-29.61	C ₁ -H ₅	-820.78	7.25×10 ⁴	-749.52
O ₂ -H ₆	-511.47	-2.86×10 ⁵	-465.17	C ₁ -H ₇	-14.33	-14.45	-14.31
F ₃ -H ₄	-31.06	-31.02	-31.26	C ₂ -F ₃	-546.94	10.18	-558.24
F ₃ -H ₆	-5.11	-5.18	-5.19	C ₂ -H ₄	-17.73	-17.99	-17.87
H ₄ -H ₅	-11.89	-13.77	-11.64	C ₂ -H ₅	-15.64	-15.90	-15.82
H ₄ -H ₆	-0.47	-0.47	-0.47	C ₂ -H ₇	-804.65	2.30×10 ⁵	-740.40
CH₃CF₃				F ₃ -H ₄	-2.92	-2.90	-2.90
C ₁ -H ₂	-818.30	8.69×10 ⁴	-746.71	F ₃ -H ₅	-3.47	-3.54	-3.54
C ₁ -C ₅	-735.49	-846.24	-758.72	F ₃ -H ₇	-31.02	-31.13	-31.29
C ₁ -F ₆	-31.84	-33.40	-33.56	H ₄ -H ₅	-15.48	-21.10	-15.16
H ₂ -H ₃	-13.27	-16.44	-13.01	H ₄ -H ₇	-1.07	-1.06	-1.06
H ₂ -C ₅	-16.37	-16.79	-16.80	H ₅ -H ₆	-15.14	-20.32	-14.82
H ₂ -F ₆	-2.55	-2.53	-2.53	H ₅ -H ₇	-1.18	-1.17	-1.17
H ₂ -F ₇	-3.45	-3.53	-3.21	H ₅ -H ₈	-2.08	-2.08	-4.90
C ₅ -F ₆	-469.52	-792.76	-488.98	H ₇ -H ₈	-13.54	-17.74	-13.22
F ₆ -F ₇	-83.69	-93.89	-93.53				

Table 4: Representative xc interaction energies (kJ/mol) for the systems of Fig. 4 (cont).

$A - B$	$(V_{xc}^{AB})_{lr,cdq}$	$(V_{xc}^{AB})_{lr}$	V_{xc}^{AB}	$A - B$	$(V_{xc}^{AB})_{lr,cdq}$	$(V_{xc}^{AB})_{lr}$	V_{xc}^{AB}
CH₃CH₂Li				CH₃NH₂			
C ₁ -C ₂	-789.95	9.49×10^3	-798.97	C ₁ -N ₂	-740.43	1.21×10^3	-753.96
C ₁ -Li ₃	-1.66	-1.67	-1.67	C ₁ -H ₃	-806.63	1.18×10^4	-740.54
C ₁ -H ₄	-810.07	1.51×10^5	-743.11	C ₁ -H ₄	-809.44	9.59×10^4	-741.04
C ₁ -H ₅	-815.31	2.79×10^5	-746.34	C ₁ -H ₆	-6.68	-7.10	-6.60
C ₁ -H ₇	-21.37	-22.48	-21.68	N ₂ -H ₃	-29.22	-29.36	-28.96
C ₂ -Li ₃	-100.43	-554.91	-96.79	N ₂ -H ₄	-27.42	-27.66	-27.76
C ₂ -H ₄	-19.31	-36.64	-18.43	N ₂ -H ₆	-770.22	1.45×10^6	-707.83
C ₂ -H ₅	-18.60	-13.76	-18.54	H ₃ -H ₄	-16.11	-21.94	-15.75
C ₂ -H ₇	-838.53	3.78×10^6	-767.82	H ₃ -H ₆	-0.59	-0.58	-0.58
Li ₃ -H ₄	-0.57	-0.57	-0.57	H ₄ -H ₅	-15.88	-22.49	-15.48
Li ₃ -H ₅	-0.16	-0.16	-0.16	H ₄ -H ₆	-0.62	-0.61	-0.61
Li ₃ -H ₇	-1.98	-1.98	-1.96	H ₄ -H ₇	-1.91	-1.90	-1.77
H ₄ -H ₅	-18.94	-36.17	-18.51	H ₆ -H ₇	-5.87	-16.69	-5.67
H ₄ -H ₇	-1.59	-1.57	-1.57	CH₃OH			
H ₅ -H ₆	-19.74	-36.04	-19.25	C ₁ -O ₂	-638.41	-187.46	-650.07
H ₅ -H ₇	-1.26	-1.25	-1.25	C ₁ -F ₃	-808.68	-6.14×10^3	-740.99
H ₅ -H ₈	-2.65	-2.64	-2.64	C ₁ -H ₄	-804.40	2.53×10^4	-738.45
H ₇ -H ₈	-23.12	-97.48	-22.57	C ₁ -H ₆	-3.79	-3.81	-3.78
CH₃CLi₃				O ₂ -F ₃	-36.31	-36.22	-36.71
C ₁ -H ₂	-806.90	4.89×10^5	-739.52	O ₂ -H ₄	-29.92	-29.73	-30.14
C ₁ -C ₅	-823.71	2.89×10^4	-839.98	O ₂ -H ₆	-553.82	-3.09×10^5	-503.97
C ₁ -Li ₆	-2.38	-2.42	-2.41	F ₃ -H ₄	-15.27	-21.13	-14.92
H ₂ -H ₃	-20.16	-63.55	-19.70	F ₃ -H ₆	-1.32	-1.31	-1.32
H ₂ -C ₅	-25.16	-33.67	-25.04	H ₄ -H ₅	-14.69	-18.89	-14.35
H ₂ -Li ₆	-0.65	-0.64	-0.64	H ₄ -H ₆	-0.50	-0.50	-0.50
H ₂ -Li ₇	-0.43	-0.43	-0.38	C₆H₆			
C ₅ -Li ₆	-135.99	-1.03×10^5	-123.94	C ₁ -C ₂	-1043.99	-2.45×10^6	-1065.06
Li ₆ -Li ₇	-1.34	-3.02	-1.29	C ₁ -C ₃	-23.85	-26.79	-24.50
				C ₁ -C ₄	-22.49	-23.40	-23.40
				C ₁ -H ₇	-819.10	1.90×10^7	-756.10
				C ₁ -H ₈	-16.89	-18.55	-17.07
				C ₁ -H ₉	-1.73	-1.73	-1.73
				C ₁ -H ₁₀	-0.92	-0.93	-0.93
				H ₇ -H ₈	-1.84	-1.86	-1.84
				H ₇ -H ₉	-0.21	-0.21	-0.21
				H ₇ -H ₁₀	-0.05	-0.05	-0.05

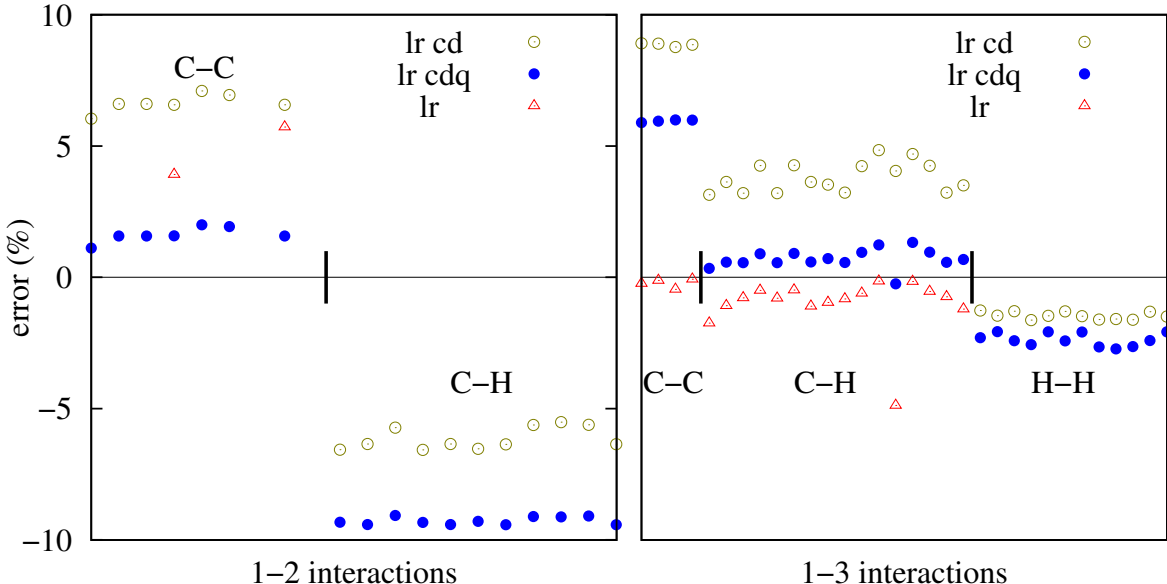
Figure 8: Relative errors, $[(V_{xc}^{AB})_{\text{method}} - (V_{xc,\text{exact}}^{AB})]/|V_{xc,\text{exact}}^{AB}| \times 100$, for the 1–2, 1–3, and 1–4 interactions of the molecules represented in Fig. 4. Empty green circles, bold blue circles, and red triangles stand for (lr,cd), (lr,cdq), and lr calculations, respectively.



by using the full lr expansion. However, they are given with reasonable accuracy by the cdq approximation. The 1– n ($n > 2$) interactions are gradually better reproduced as n increases in both the lr and cdq approximations. It is very satisfactory to check that the cdq approach, a severe truncation of the full mp expansion, is perfectly suited to simulate the xc interaction between pairs of atoms beyond the directly bonded ones. Even in typically covalent molecules like benzene all the cdq C–C xc interaction energies reproduce very well the exact values. As we can see in Fig. 8 most of the 1–2 interactions have relative cdq errors $\leq 10\%$. This improves for the 1–3 and 1–4 interactions.

Our results for the saturated hydrocarbons C_nH_{2n+2} ($n = 2 - 5$) are presented only in graphical form in Fig. 9. We find the surprising result that all 1–2 C–C cdq interactions are predicted with errors $\leq 2\%$ while the cdq energies between the more distant 1–3 C–C pairs have errors about 5–6%. Nevertheless, the interactions between even more distant C–C pairs turn again to be calculated quite accurately (errors $< 1\%$) in the cdq approximation. The lr approximation fails completely to predict the 1–2 C–C interactions, but yields negligible errors for the 1–3 xc interaction energies. With regard to the C–H interactions, the situation is the opposite of that found for the C–C pairs: 1-2 C–H cdq errors are about 9-10% (except in ethane where the error is unusually large (54%)) whereas all except two of the 1-3 C–H cdq errors are $< 1\%$. For these two exceptions the error is not too large

Figure 9: Relative errors, $[(V_{xc}^{AB})_{\text{method}} - (V_{xc,\text{exact}}^{AB})]/|V_{xc,\text{exact}}^{AB}| \times 100$, for the 1 – 2 (left) and 1 – 3 (right) interactions of the molecules represented in Fig. 5.



($\sim 1.3\%$). We observe in Fig. 9 that the cdq approximation improves considerably the cd results, giving 1-3 C–H interaction energies almost as accurate as the lr ones. Another surprising result in these systems concerns the cdq 1–3 H–H interactions: Contrary to what happens almost systematically, the cdq results are worse than the cd ones, albeit the relative errors in both approximations are acceptable ($\sim 2 - 3\%$).

The different behavior of the lr and cdq approximations can be further illustrated with the case of the phenol dimer (Fig. 6). For this system, the relative errors *versus* the interatomic distance R_{A-B} in these two approximations are plotted in Fig. 10, both for intra-molecular and inter-molecular atomic pairs. Only two points, associated to intra-molecular interactions, have a relative error (absolute value) $\geq 20\%$ in the cdq calculation, while the error for all the lr points with $R_{A-B} < 2.64$ (most of them associated to intra-molecular pairs) is larger than 20%. However, for $R_{A-B} > 5.0$ the lr approximation gives quite accurate *xc* interaction energies for all the pairs, whereas cdq errors are still important.

However, there is a general problem of the lr approximation that deserves to be commented: Eq. 15 does not necessary converges to the exact *xc* interaction for large $l_1 m_1$ and $l_2 m_2$ values. This fact is illustrated in Fig. 11, where the *xc* energies for some of the atomic

Figure 10: Relative error of the cdq (left) and lr (right) calculations for the phenol-dimer ($C_6H_5OH \cdots C_6H_5OH$). Only two (2) points are out of the ordinate scale in the cdq calculation, while all the points (26) with $R_{A-B} < 2.64$ bohr are out of the ordinate scale in the lr calculation.

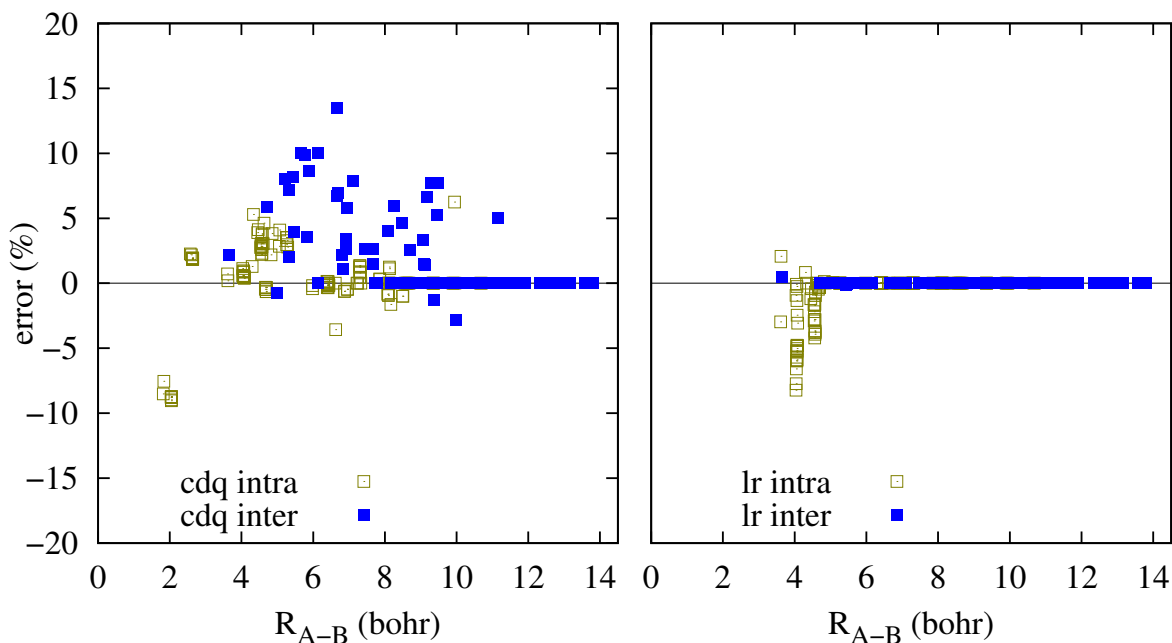


Figure 11: Convergence of the $A - B$ interactions indicated in the figure. The pairs i, j correspond to the labels of Fig. 4

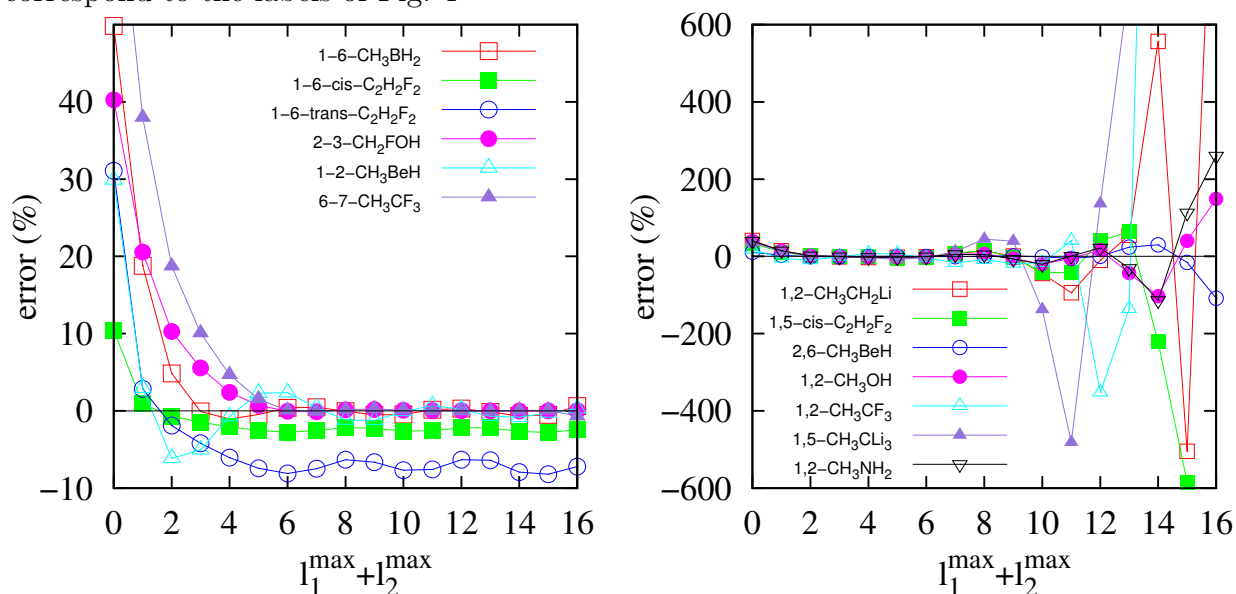
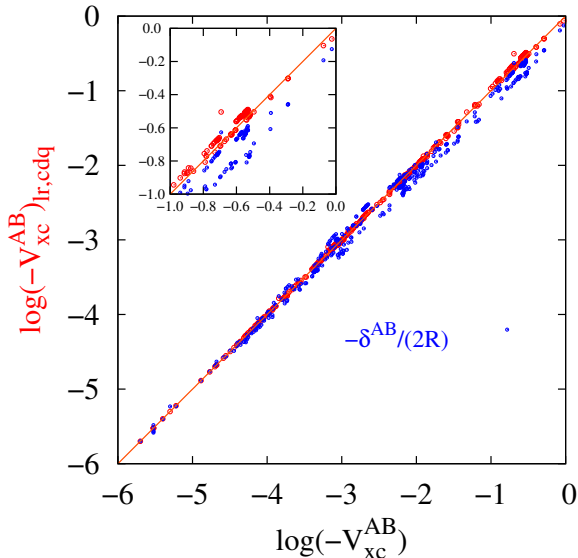


Figure 12: Comparison of all the exact V_{xc}^{AB} values considered in this work to the monopole-monopole and cdq approximations in a logarithmic scale.



pairs of the molecules in Fig. 4 are represented *versus* $l_1^{\max} + l_2^{\max}$. The lr approximation suffers a systematic error in the C_1-F_6 interaction of cis- CH_2CF_2 and trans- CH_2CF_2 molecules, regardless the value of $l_1^{\max} + l_2^{\max}$. In the case of trans- CH_2CF_2 the C_1-F_6 xc interaction energy shows an oscillating behavior around an (erroneous) mean value. This pattern has been also observed in many other cases. Contrarily, as we have repeatedly said in this section, catastrophic lr interactions (see, for instance Fig. 11) are still reasonable provided that the sum $l_1 + l_2$ is interrupted at a value approximately in the interval $2 \leq l_1 + l_2 \leq 6$.

Summarizing, we have shown that the multipole series for the interatomic xc energies is conditionally convergent, and that the computational burden of the quasi-exact calculation of V_{xc} when general QTAIM domains are used may be ameliorated by retaining up to quadrupole-quadrupole terms. With this approximation, reasonable errors are obtained in the medium- to long-distance range, sometimes even for directly bonded interactions. An overall image of the improvement of the cdq approximation over the cc (monopole-monopole) one can be grasped from Fig. 12 that condenses all our calculations that span a six orders of magnitude range for V_{xc} .

CONCLUSIONS

We have shown that the interatomic exchange-correlation energies used in real space theories of chemical bonding, which measure the covalent contribution to a given interatomic interaction, can be approximated via a conventional multipole expansion. Rigorously, the series diverges when atoms are directly bonded, although it may be regarded asymptotically convergent. Truncation of the series up to $l_1 + l_2 = 2$ (including up to charge-quadrupole interactions) tends to provide results which are accurate to a few per for 1- n , $n > 2$ interactions, and even to about 10% in many 1-2 directly bonded cases.

Since the computational burden needed to calculate the multipole series is considerably smaller than that of the exact bipolar expansion, our results may be important to estimate covalent interactions in those cases where exact integrations are not feasible. They can also be used to ameliorate the computational cost in IQA decompositions of large systems, where many expensive, but small long-range xc terms can now be safely approximated without loss of precision.

APPENDIX

We derive in this appendix Eq. 15, the multipolar approximation to the exact exchange-correlation interaction, Eqs. 10 and 11. Further details are given in I. We start by using the bipolar expansion for r_{12}^{-1} ,

$$r_{12}^{-1} = \sum_{l_1 m_1}^{\infty} \sum_{l_2 m_2}^{\infty} S_{l_1 m_1}(\hat{r}_1) S_{l_2 m_2}(\hat{r}_2) D_{l_1 m_1}^{l_2 m_2}(r_1, r_2, \mathbf{R}), \quad (24)$$

where $\mathbf{r}_1 \equiv (r_1, \hat{r}_1)$ and $\mathbf{r}_2 \equiv (r_2, \hat{r}_2)$ are referred to centers A and B, respectively, $\mathbf{R} = (\mathbf{R}_B - \mathbf{R}_A) \equiv (R, \hat{R})$ is the vector position of center B with respect to center A (see Fig. 13),

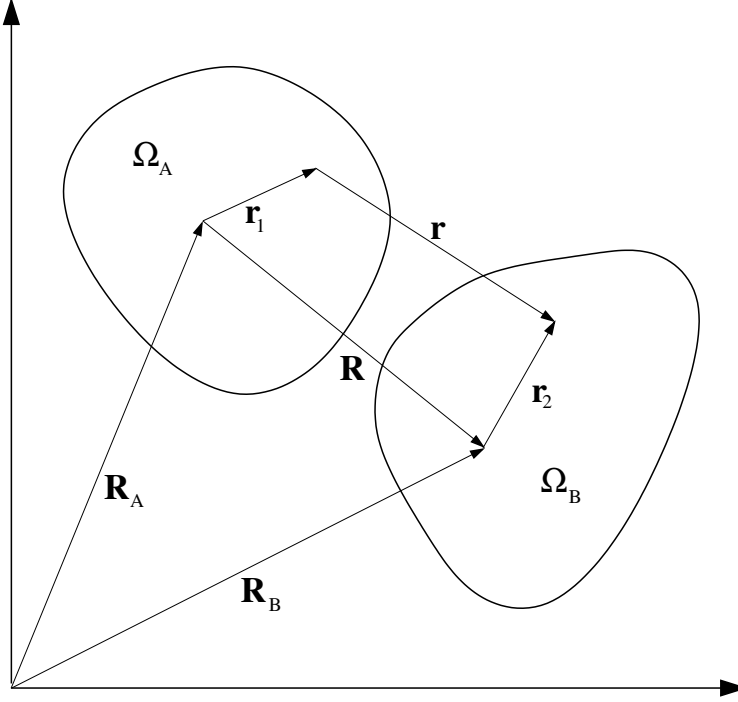


Figure 13: Coordinate System

$S_{lm}(\hat{r})$ are real spherical harmonics defined as³²

$$S_{lm}(\theta, \phi) = \Theta_{l|m|}(\theta)\Phi_m(\phi), \quad (25)$$

$$\Theta_{lm}(\theta) = \sqrt{\frac{2l+1}{4\pi} \frac{(l-|m|)!}{(l+|m|)!}} P_l^m(\cos\theta), \quad (26)$$

$$\Phi_m(\phi) = \begin{cases} \sqrt{2} \cos m\phi & m > 0, \\ 1 & m = 0, \\ \sqrt{2} \sin |m|\phi & m < 0, \end{cases} \quad (27)$$

and $P_l^m(\cos\theta)$ are the associated Legendre functions, defined for $m \geq 0$ by

$$P_l^m(x) = \frac{1}{2^l l!} (1-x^2)^{m/2} \frac{d^{l+m}}{dx^{l+m}} (x^2-1)^l. \quad (28)$$

Finally, $D_{l_1 m_1}^{l_2 m_2}(r_1, r_2, \mathbf{R})$ in eq. 24 is defined as

$$D_{l_1 m_1}^{l_2 m_2}(r_1, r_2, \mathbf{R}) = 4\pi (-1)^{l_1} \sum_{l_3=|l_1-l_2|}^{l_1+l_2} \mathcal{V}_{l_1 l_2 l_3}(r_1, r_2, R) T_{l_1 m_1 l_2 m_2}^{l_3}(\hat{R}), \quad (29)$$

where the sum over l_3 runs in steps of 2, $\mathcal{V}_{l_1 l_2 l_3}(r_1, r_2, R)$ is a discriminant that takes different

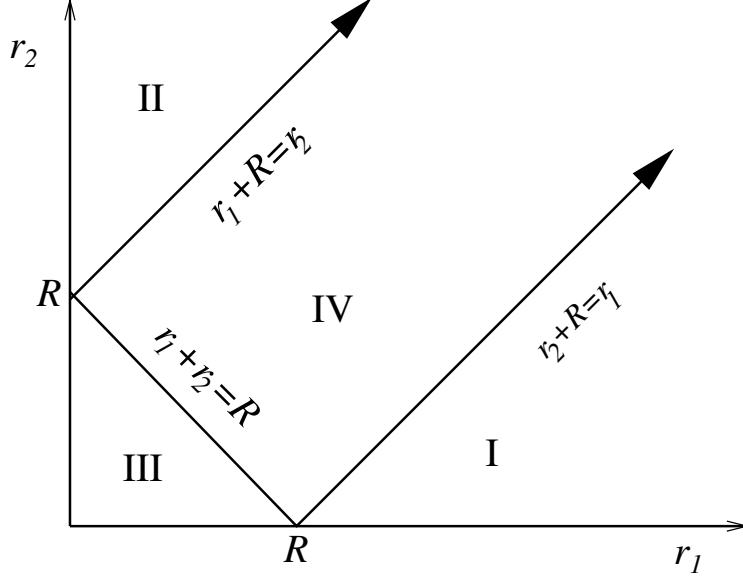


Figure 14: Regions of definition of the $\mathcal{V}_{l_1 l_2 l_3}(r_1, r_2, R)$ function

expressions in the four regions defined in Fig. 14, and $T_{l_1 m_1 l_2 m_2}^{l_3}(\hat{R})$ is the angular factor

$$T_{l_1 m_1 l_2 m_2}^{l_3}(\hat{R}) = \sum_{m_3=-l_3}^{+l_3} d_{l_1 m_1 l_2 m_2}^{l_3 m_3} S_{l_3 m_3}(\hat{R}), \quad (30)$$

where $d_{l_1 m_1 l_2 m_2}^{l_3 m_3}$ is the Gaunt coefficient between the $S_{lm}(\theta, \phi)$'s defined by

$$d_{l_1 m_1 l_2 m_2}^{l_3 m_3} = \langle S_{l_3 m_3} | S_{l_1 m_1} | S_{l_2 m_2} \rangle. \quad (31)$$

Given that S_{lm} is real, $d_{l_1 m_1 l_2 m_2}^{l_3 m_3}$ is invariant against any permutation of the pair of indices (l_i, m_i) . These coefficients may be determined as described elsewhere. Using Eq. 24 in Eq. 11 one has

$$K_{ij}^{AB} = \sum_{l_1 m_1} \sum_{l_2 m_2} \int_{\Omega_A} S_{l_1 m_1}(\hat{r}_1) f_{ij}(\mathbf{r}_1) d\mathbf{r}_1 \int_{\Omega_B} S_{l_2 m_2}(\hat{r}_2) f_{ij}(\mathbf{r}_2) d\mathbf{r}_2 D_{l_1 m_1}^{l_2 m_2}(r_1, r_2, \mathbf{R}). \quad (32)$$

A further simplification of K_{ij}^{AB} requires the explicit form of $D_{l_1 m_1}^{l_2 m_2}(r_1, r_2, \mathbf{R})$. From the expression of $\mathcal{V}_{l_1 l_2 l_3}(r_1, r_2, R)$ (Eqs. (B1)-(B9) of I) it follows that, as long as $r_1 + r_2 \leq R$, this discriminant only takes a nonzero value in region III of the (r_1, r_2) space (see Fig. 14). This condition will be exactly satisfied if $R \geq r_1^{\max} + r_2^{\max}$, where r_1^{\max} is the maximum value of the radial coordinate within Ω_A , with an equivalent definition for r_2^{\max} . In the present context, atoms A and B are said to be non-overlapping if this condition is fulfilled, and

overlapping otherwise. Although it may occur that the condition $R \geq r_1^{\max} + r_2^{\max}$ is not exactly satisfied, provided that the atomic basins Ω_A and Ω_B are well-separated in the space, we can expect that it is fulfilled in practical terms. The multipolar approach, intensively used to approximate the Coulomb repulsion in the modellization of biomolecules, is equivalent to the assumption that $r_1 + r_2 \leq R$ for any r_1 and r_2 . Thus, region III is identified with the complete first quadrant. In this region, $D_{l_1 m_1}^{l_2 m_2}(r_1, r_2, \mathbf{R})$ is given by

$$D_{l_1 m_1}^{l_2 m_2}(r_1, r_2, \mathbf{R}) = (-1)^{l_1} 16\pi^2 \Delta_{l_1 l_2} \frac{r_1^{l_1} r_2^{l_2}}{R^{l_1+l_2+1}} T_{l_1 m_1 l_2 m_2}^{l_1+l_2}(\hat{R}), \quad \text{where} \quad (33)$$

$$\Delta_{l_1 l_2} = (-1)^{l_1+l_2} \frac{(2l_1 + 2l_2)! l_1! l_2!}{(l_1 + l_2)! (2l_1 + 1)! (2l_2 + 1)!}. \quad (34)$$

Using Eq. 33 in Eq. 32 we get

$$(K_{ij}^{AB})_{\text{lr}} = \sum_{l_1 m_1} \sum_{l_2 m_2} C_{l_1 m_1 l_2 m_2}(\hat{R}) \frac{q_{ij, l_1 m_1}^{\Omega_A} q_{ij, l_2 m_2}^{\Omega_B}}{R^{l_1+l_2+1}}, \quad \text{where} \quad (35)$$

$$C_{l_1 m_1, l_2 m_2}(\hat{R}) = (-1)^{l_1} 4\pi [(2l_1 + 1)(2l_2 + 1)]^{\frac{1}{2}} \Delta_{l_1 l_2} T_{l_1 m_1 l_2 m_2}^{l_1+l_2}(\hat{R}), \quad (36)$$

and the $q_{ij, lm}^{\Omega}$ have been defined in Eq. 17. Finally, substituting Eq. 35 in Eq. 10 we obtain Eq. 15, the multipolar approximation for the exchange-correlation interaction, $(V_{\text{xc}}^{AB})_{\text{lr}}$.

ACKNOWLEDGEMENTS

The authors thank the Spanish MINECO/FEDER, grant CTQ2015-65790-P, for financial support.

References

1. S. Kurth and J. P. Perdew, *Int. J. Quant. Chem.* **77**, 814 (2000).
2. W. Kohn and L. J. Sham, *Phys. Rev.* **140**, A1133 (1965).
3. E. J. Baerends and O. V. Gritsenko, *J. Phys. Chem. A* **101**, 5383 (1997).
4. E. Francisco, A. Martín Pendás, and M. A. Blanco, *J. Chem. Theory Comput.* **2**, 90 (2006).

5. E. Francisco, A. Martín Pendás, and M. A. Blanco, *J. Chem. Theory Comput.* **2**, 90 (2006).
6. A. Martín Pendás, M. A. Blanco, and E. Francisco, *J. Comput. Chem.* **28**, 161 (2007).
7. M. Kohout, *Int. J. Quant. Chem.* **97**, 651 (2004).
8. M. Causà and A. Savin, *J. Phys. Chem. A* **115**, 13139 (2011).
9. B. M. Gimarc, *Molecular structure and bonding. The qualitative molecular orbital approach* (Academic Press, New York, 1979).
10. R. F. W. Bader, *Atoms in Molecules* (Oxford University Press, Oxford, 1990).
11. A. D. Becke and K. E. Edgecombe, *J. Chem. Phys.* **92**, 5397 (1990).
12. B. Silvi and A. Savin, *Nature* **371**, 683 (1994).
13. P. L. A. Popelier and E. A. Brèmond, *Int. J. Quant. Chem.* **109**, 2542 (2009).
14. A. Martín Pendás, E. Francisco, and M. A. Blanco, *J. Phys. Chem. A* **110**, 12864 (2006).
15. J. M. Guevara-Vela, C.-C. R., M. García-Revilla, J. Hernández Trujillo, O. Christiansen, E. Francisco, A. Martín Pendás, and T. Rocha-Rinza, *Chem. Eur. J.* **19**, 4304 (2013).
16. C. Gatti and P. Macchi, eds., *Modern Charge-density Analysis* (Springer, Dordrecht., 2012).
17. R. Chauvin, C. Lepetit, B. Silvi, and E. Alikhani, eds., *Applications of Topological Methods in Molecular Chemistry* (Springer Intl., 2016).
18. A. Martín Pendás, E. Francisco, M. A. Blanco, and C. Gatti, *Chem. Eur. J.* **13**, 9362 (2007).
19. M. García-Revilla, P. L. A. Popelier, E. Francisco, and A. Martín Pendás, *J. Chem. Theory Comput.* **7**, 1704 (2011).
20. E. Bartashevich, E. Troitskaya, A. Martín Pendás, and V. G. Tsirelson, *Comput. Theor. Chem.* **1053**, 229 (2015).

21. E. Bartashevich, A. Martín Pendás, and V. G. Tsirelson, *Phys. Chem. Chem. Phys.* **16**, 16780 (2014).
22. A. Martín Pendás, M. A. Blanco, and E. Francisco, *J. Comput. Chem.* **30**, 98 (2009).
23. M. García-Revilla, E. Francisco, P. L. A. Popelier, and A. Martín Pendás, *ChemPhysChem* **14**, 1211 (2013).
24. R. F. W. Bader and M. E. Stephens, *Chem. Phys. Lett.* **26**, 445 (1974).
25. K. B. Wiberg, *Tetrahedron* **24**, 1083 (1968).
26. I. Mayer, *Chem. Phys. Lett.* **270**, 97 (1983).
27. M. Rafat and P. L. A. Popelier, in *The Quantum Theory of Atoms in Molecules. From Solid State to DNA and Drug Design*, edited by C. F. Matta and R. J. Boyd (Wiley-VCH, 2007), p. 121.
28. E. Francisco and A. Costales, *Comput. Theor. Chem.* **1053**, 77 (2015).
29. A. Martín Pendás, E. Francisco, and M. A. Blanco, *J. Comput. Chem.* **26**, 344 (2005).
30. A. Martín Pendás, M. A. Blanco, and E. Francisco, *J. Chem. Phys.* **120**, 4581 (2004).
31. A. Martín Pendás and E. Francisco, a QTAIM/IQA code (Available from the authors upon request).
32. C. D. H. Chisholm, *Group Theoretical Techniques in Quantum Chemistry* (Academic Press, London, 1976), ISBN 0-12-172950-8.